Proc. Natl. Acad. Sci. USA
Vol. 83, pp. 8987–8991, December 1986
Biophysics

Temporal comparisons in bacterial chemotaxis

(impulse response/step response/adaptation/gain)

JEFFREY E. SEGALL*†, STEVEN M. BLOCK*‡, AND HOWARD C. BERG*§

*Division of Biology 216-76, California Institute of Technology, Pasadena, CA 91125

Contributed by Howard C. Berg, August 18, 1986

ABSTRACT **Responses of tethered cells of *Escherichia coli* to impulse, step, exponential-ramp or exponentiated sine-wave stimuli are internally consistent, provided that allowance is made for the nonlinear effect of thresholds. This result confirms that wild-type cells exposed to stimuli in the physiological range make short-term temporal comparisons extending 4 sec into the past: the past second is given a positive weighting, the previous 3 sec are given a negative weighting, and the cells respond to the difference. cheRcheB mutants (defective in methylation and demethylation) weight the past second in a manner similar to the wild type, but they do not make short-term temporal comparisons. When exposed to small steps delivered iontophoretically, they fail to adapt over periods of up to 12 sec; when exposed to longer steps in a flow cell, they partially adapt, but with a decay time of >30 sec. cheZ mutants use a weighting that extends at least 40 sec into the past. The gain of the chemotactic system is large: the change in occupancy of one receptor molecule produces a significant response.**

Flagellated bacteria, such as *Escherichia coli*, possess a stimulus–response system in which the input is the local concentration of a chemical and the output is the motion of the cell. Some chemicals, such as aspartate, are sensed by specific receptors (1). Changes in their occupancy lead to changes in the probability that the flagella spin clockwise (CW) or counterclockwise (CCW). This determines whether the cell moves erratically with little net displacement (tumbles) or swims smoothly (runs), respectively (2, 3). These modes alternate, causing the cell to move about as in a random walk (4). When the occupancy of the aspartate receptor increases, the probability of CCW rotation increases, the flagella tend to remain in a bundle that pushes the cell forward, and the cell continues to run. Thus, in a spatial gradient of attractant, the random walk is biased: runs that happen to carry the cell up the gradient are extended. This enables the cell to move to a more favorable environment.

The aspartate receptor is a protein of $M_r \approx 60{,}000$ that spans the cytoplasmic membrane (for a review of the genetics and biochemistry of bacterial chemotaxis, see ref. 5). It has at least one ligand binding site in its periplasmic domain and several methylation sites in its cytoplasmic domain. When the time-averaged occupancy of the binding site increases, a signal is sent to the flagella that raises the rotational bias (the probability that the motors spin CCW). The nature of this signal is not known; however, it is turned off or its effect is counteracted by receptor methylation. The methylation is catalyzed by a transferase, the product of the *cheR* gene. When the occupancy of the binding site decreases, the methyl groups are removed by an esterase, the product of the *cheB* gene. Several other cytoplasmic proteins are involved in this process, including the products of the *cheA*, *cheW*, *cheY*, and *cheZ* genes. Their functions are poorly understood. However, defects in any of these genes have profound effects on bacterial behavior.

A variety of methods have been used to monitor the chemotactic behavior of wild-type and mutant bacterial strains. The simplest involves observation of chemotactic rings on agar plates; however, ring formation requires transport, metabolism, and growth, in addition to chemotaxis (6). Another method involves the addition of a large amount of an attractant or a repellent to a population of swimming (or tethered) cells. These respond by swimming smoothly or tumbling (or spinning CCW or CW) for a relatively long period of time and then they eventually recover (2, 7). In wild-type cells, the time required for recovery is proportional to the net change in receptor occupancy (8, 9). A third method follows the accumulation of cells in capillary tubes containing attractants at different concentrations (10). Some other methods are less convenient but provide additional information. These include measurements of drift rates of cells in layered gradients (11, 12) and three-dimensional tracking of cells in spatial gradients near capillary tubes (4) or in temporal gradients generated by enzymatic reaction (13). Recently, we studied the responses of tethered cells to pulses or small steps of attractants or repellents delivered iontophoretically (14) or to gradual changes in concentration produced by programmed mixing (15). These experiments were designed to probe chemotactic behavior at the level of a single flagellar motor under conditions in which the response does not saturate.

Wild-type cells of *E. coli* respond to a pulse of an attractant by changing the rotational bias of their flagellar motors in a biphasic manner, as shown in Fig. 1. Smaller impulses produce smaller responses, but they follow the same time course (14). Measurements of the impulse response are useful, because, in principle, they allow one to predict the response of a tethered cell to an arbitrary stimulus: any temporal change in concentration can be represented as a series of impulses of appropriate size, and the response to that change can be found by summing the corresponding series of impulse responses. Such predictions work provided that the system is linear—e.g., that there are no thresholds and the stimulus does not saturate the response. Experiments with cells exposed to exponential ramp or exponentiated sine-wave stimuli—stimuli that generate linear or sine-wave changes in receptor occupancy—indicate that thresholds for addition of attractant are small, while those for removal of attractant are relatively large (15). However, once these thresholds are crossed, the response appears to be linear: equal increments in ramp rate or frequency generate equal increments in rotational bias until saturation occurs.

We now have compared the results of impulse, small-step, ramp, and sine-wave experiments and have found them to be

The publication costs of this article were defrayed in part by page charge payment. This article must therefore be hereby marked "*advertisement*" in accordance with 18 U.S.C. §1734 solely to indicate this fact.

Abbreviations: CW, clockwise; CCW, counterclockwise.

†Present address: Max-Planck-Institut für Biochemie, 8033 Martinsried bei München, Federal Republic of Germany.
‡Present address: Department of Cell Biology, Stanford University School of Medicine, Stanford, CA 94305.
§To whom requests for reprints should be addressed.

internally consistent. Data are presented on the behavior of wild-type cells and of mutants defective in methylation and demethylation (deleted for *cheR* and *cheB*) or in the functions specified by *cheY* or *cheZ*.

RESULTS

Calibration of the Impulse Response. Given the impulse response of Fig. 1 (induced by pulses of small but unknown amplitude), one can predict the time course of the response to an arbitrary stimulus; however, the amplitude of this response is unknown up to a constant scaling factor. To predict both the amplitude and the time course of a response, this scaling factor must be determined. First, we measured the rate at which attractant was released from a particular set of pipettes by exposing cells 5 μm away to a large step in current (−100 nA) and recording their recovery times: this works because the steady-state concentration of attractant a fixed distance away from the tip of a pipette is proportional to the rate of release (p. 23 of ref. 17), and the recovery time is proportional to the net change in receptor occupancy (cf. table 1 of ref. 16). Next, we measured the amplitude of the response of the same cells to a smaller step in current (−3 to −10 nA). Assuming that the rate of release varies linearly with current, the change in concentration generated by the smaller step was determined. The type of response generated by the smaller steps is shown in Fig. 2. Note that this response is not saturated. For the subset of cells used in the calibration (those exposed to α-methyl-DL-aspartate; see figure legend) a change in bias of 0.23 occurred for an estimated change in fraction of receptor bound of 0.0042. Finally, we calibrated the impulse response by subtracting the baseline and scaling its integral to the change in bias of the calibrated step response. We found that a response of the amplitude shown in Fig. 1 would be generated by a pulse that increased the receptor occupancy by 0.19 for a period of 20 msec (the approximate width of the shortest pulse used in our experiments).

Comparisons with Ramp and Sine-Wave Data. The solid line in Fig. 3*A* is the dependence of bias on ramp rate for experiments involving linear changes in receptor occupancy

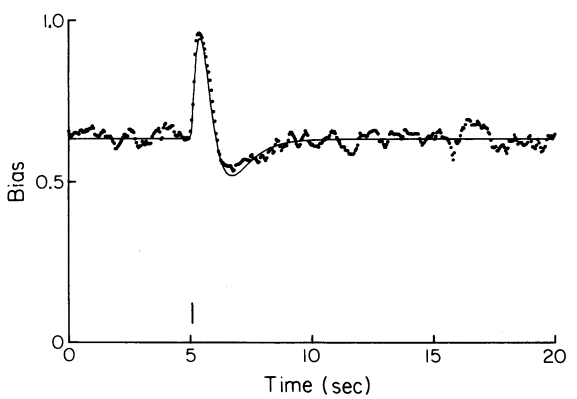

FIG. 1. Impulse response to attractant in wild-type cells. The dotted curve is the probability, determined from repetitive stimulation, that tethered cells of strain AW405 spin CCW when exposed to pulses of L-aspartate or α-methyl-DL-aspartate beginning at 5.06 sec (vertical bar). The smooth curve is a fit to a sum of exponentials (see text). For methods, see refs. 14 and 16. Pipettes containing aspartate (1 mM) were pulsed for 0.02 sec at −25 to −100 nA, and pipettes containing methylaspartate (1–3 mM, with 1.6 mM in the bath) were pulsed for 0.12 sec at −100 nA, both at 32°C. Some pipettes containing 1–7 mM methylaspartate were pulsed for 0.03–0.12 sec at −50 to −100 nA at 22°C. The curve was constructed from 378 records comprising 7566 reversals of 17 cells. Points were determined every 0.05 sec.

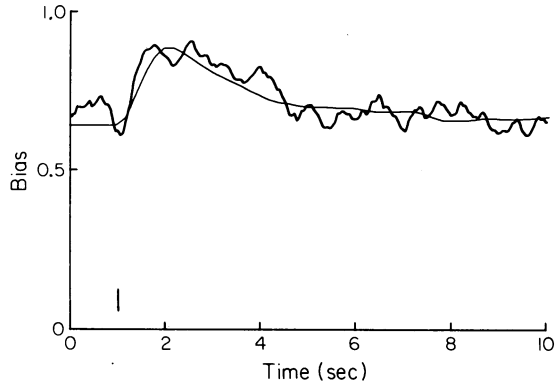

FIG. 2. Step response to attractant in wild-type cells. The thick curve is the probability that cells of strain AW405 spin CCW when exposed to steps of L-aspartate or α-methyl-DL-aspartate beginning at 1.00 sec (vertical bar). Pipettes containing aspartate (0.1–1.0 mM) or methylaspartate (1–10 mM, with 1.6 mM in the bath) were switched on for 12 sec at −3 to −10 nA at 32°C. The curve was constructed from 227 records comprising 5040 reversals of 10 cells and was plotted as described in Fig. 1. The thin line is the response predicted from the impulse response (the dotted curve) of Fig. 1 (cf. figure 4 of ref. 14). Note the expanded time scale.

predicted by the impulse response; the dashed line has the same slope but is offset 0.0015 to compensate for the response threshold. The slope of the predicted dependence is 114 sec, while a linear least-squares fit to the data gave a mean slope and standard deviation of 78 ± 18 sec. Note that a shift in bias of 0.1 occurs for a ramp that increases the receptor occupancy by ≈0.1% per sec. The solid line in Fig. 3*B* is the spectral response to sinusoidal changes in receptor occupancy at different frequencies derived from the fit to the impulse response (the smooth curve) of Fig. 1; the points comprise a similar prediction based on the data (the dotted curve) of Fig. 1. The stars are the peak-to-peak changes in bias observed for sinusoidal oscillations in receptor occupancy generated by programmed mixing (figure 7 of ref. 15). Use of the latter measure assumes a large response threshold for negative rates of change of receptor occupancy (figure 6*B* of ref. 15). The close agreement between the Fourier transform represented by the solid line in Fig. 3*B* and the data at very low frequency is not fortuitous: the fit to the sum of exponentials (the smooth curve of Fig. 1) was constrained so that its Fourier transform passed through the point (−3, 0.75). Figs. 1 and 3*B* together show that the impulse and sine-wave data are consistent. With allowance for thresholds, the agreement between the three different sets of measurements is satisfactory.

Impulse and Step Responses of Mutant Cells. As reported earlier (figure 7*A* of ref. 14), cells with deletions in genes for the methyltransferase (*cheR*) and the methylesterase (*cheB*) show impulse responses with the second lobe much reduced (Fig. 4*A*). This implies that such cells cannot adapt over a short time span to a sudden increase in the concentration of attractant. The measured step response bears out this prediction (Fig. 4*B*). We also studied the behavior of *cheRcheB* cells over a longer time span in a flow cell (19). Some cells failed to respond to step stimuli (shifts from 0 to 25 μM L-aspartate or from 0 to 1 mM α-methyl-DL-aspartate); others spun exclusively CCW and failed to recover; still others gave a sizable response and then partially recovered (Fig. 5). Some of the latter cells exhibited dramatic swings in bias over periods of the order of 1 min, but no periodicity was evident in the average (Fig. 5). Note that *cheRcheB* cells are less sensitive to L-aspartate or to α-methyl-DL-aspartate than wild-type cells by factors of 10–100.

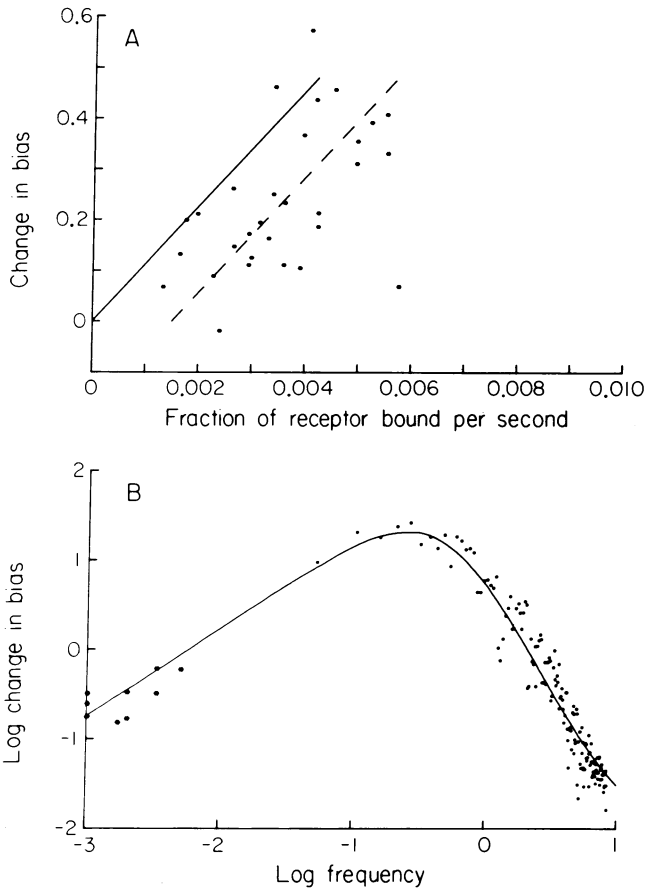

FIG. 3. Comparison of impulse and ramp data in the time (*A*) and frequency (*B*) domain for wild-type cells stimulated with α-methyl-DL-aspartate. (*A*) Change in bias as a function of ramp rate, expressed as the time rate of change of fraction of receptor bound. Data points are from the ramp experiments (figure 6*A* of ref. 15 and unpublished data). The solid line is the prediction based on the calibrated impulse response. The dashed line is this curve shifted to the right to compensate for the threshold. (*B*) The logarithm (base 10) of the change in bias as a function of the logarithm of the stimulus frequency. Data points on the left were obtained from the sine-wave experiments of ref. 15 (from changes in bias observed during the rising phase of receptor occupancy). Data points on the right are the absolute magnitude of the complex Fourier transform of the impulse response (the dotted curve) of Fig. 1 (cf. ref. 14). The line is a similar transform of the smooth curve of Fig. 1.

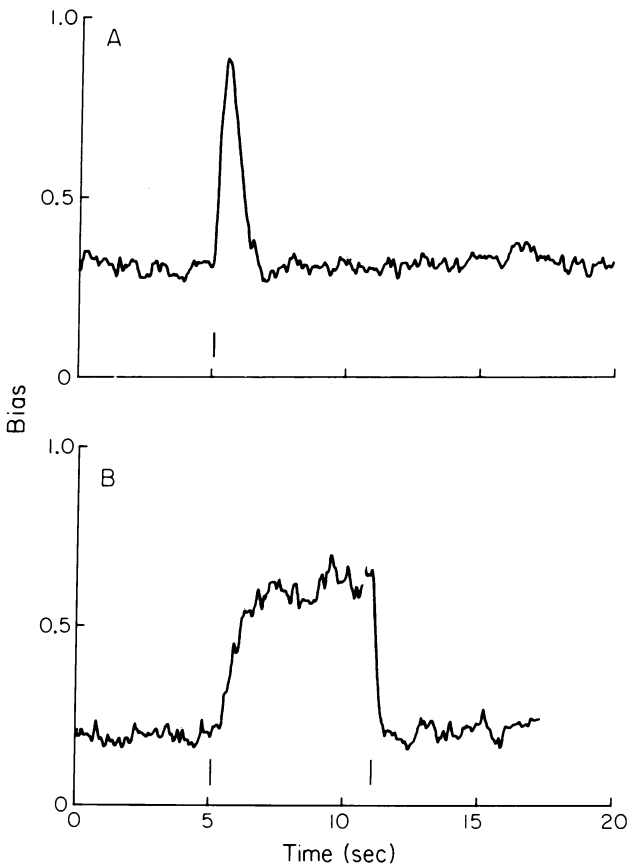

FIG. 4. Impulse (*A*) and step (*B*) responses to attractant in strains deleted for *cheRcheB* (18). (*A*) Cumulative responses of cells of strains RP2867 (*tap*$^-$) and RP4969 (*tap*$^+$) to pulses of L-aspartate beginning at 5.06 sec (vertical bar). Pipettes containing aspartate (3–20 mM) were pulsed for 0.01–0.39 sec at −50 to −100 nA at 22°C or 32°C. The curve was constructed from 207 records comprising 5006 reversals of 13 cells and was plotted as described in Fig. 1. (*B*) Cumulative responses of cells of strain RP2867 to steps of L-aspartate beginning at 5.06 sec (left vertical bar) and ending 5–12 sec later (right vertical bar). The responses to the ends of the steps are shown beginning at 10.6 sec (at the break in the curve). Pipettes containing aspartate (3–20 mM) were switched on at −3 to −20 nA at 32°C. The curves were constructed from 178 records comprising 5184 reversals of six cells and were plotted as described in Fig. 1.

The impulse response for cheZ and cheZcheC double mutants, when examined over a longer time span than before (cf. figure 7*B* of ref. 14), proved to be biphasic; however, the second lobe had a smaller area than the first (Fig. 6*A*). As predicted from such an impulse response, the step response rose to a maximum in ≈10 sec and then gradually dropped toward its initial value, failing to reach that value over the longest periods tested (Fig. 6*B*, top curve). The response to the removal of the step showed similar kinetics.

cheY mutants (20) proved difficult to excite: cells of strains RP2768 (*cheY201*) and RP2770 (*cheY220*) failed to respond to the repellent Ni^{2+}, but those of strain RP4838 (*cheY216*) gave a response similar to the *cheRcheB* strain but inverted (cf. figure 3*B* of ref. 14). Since these cells rotated exclusively CCW in the absence of a stimulus, we could not determine whether the response was biphasic. Strains containing mutations in *cheA* or *cheW* also rotated exclusively CCW; they did not respond to Ni^{2+}.

Transition Rates. A complete description of cell behavior requires specification of the rates at which transitions occur between CW and CCW states (14). In general, these rates

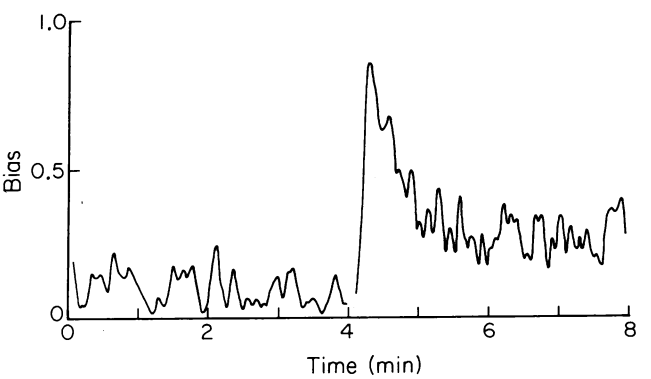

FIG. 5. Step response to attractant (1 mM α-methyl-DL-aspartate) in a strain deleted for *cheRcheB* (RP2867). The stimulus was delivered by bulk flow for a period of 10 sec beginning at 4 min, as indicated by the break in the curve. The curve was constructed from 10 records comprising 1742 reversals of eight cells, by computing the mean bias over a 20-sec interval every 2 sec. Similar results were obtained with 25 μM L-aspartate (data not shown). The cells were grown in tryptone broth and then washed and tethered as described (15). The experiments were done at room temperature.

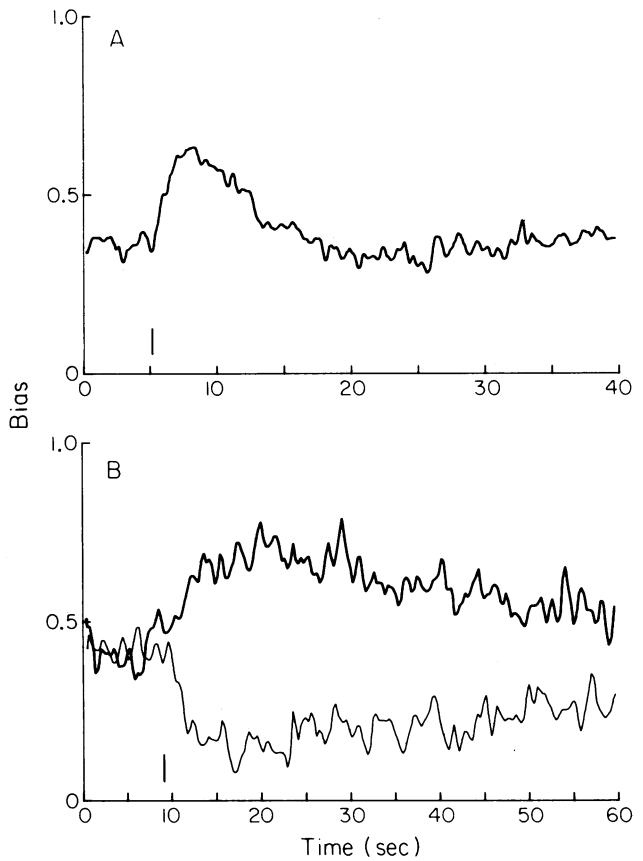

FIG. 6. Impulse (*A*) and step (*B*) responses to attractant in cheZ mutants (20, 21). (*A*) Cumulative responses of cells of strains RP5006 (*cheZ292* amber), RP5007 (*cheZ293*), and RP2734 (*cheZ280 cheC183*) to pulses of L-aspartate beginning at 5.06 sec (vertical bar). Pipettes containing aspartate (0.3 or 1.0 mM) were pulsed for 0.67–1.24 sec at −100 nA at 32°C. The curve was constructed from 175 records comprising 13,653 reversals of six cells. The mean bias in a 0.6-sec window was calculated and plotted every 0.3 sec. Note: the *cheC* mutation was introduced to raise the prestimulus bias; the impulse responses of cheZ and cheZcheC mutants appeared to have similar time courses. (*B*) Cumulative responses of cells of strain RP5007 to steps of L-aspartate beginning at 9.06 sec (vertical bar, top curve) and lasting ≈50 sec or ending at 9.06 sec (vertical bar, bottom curve). The bottom curve was shifted downward 0.17. Pipettes containing aspartate (0.1 or 0.2 mM) were switched on at −8 to −20 nA at 22°C. The curves were constructed from 53 records comprising ≈6000 reversals of three cells and were plotted as described in *A*. Note the different time scales.

change smoothly in an antagonistic manner. Their initial and extreme values for the present set of experiments are given in Table 1. The essential point here is that the stimuli that we used still allowed CCW-to-CW transitions to occur at rates of 0.1 sec^{-1} or higher. For example, the mean CCW interval observed for the first 20 sec following addition of attractant to the flow cell (Fig. 5) was 4.2 sec; the mean CW interval was 1.4 sec.

DISCUSSION

The impulse response of Fig. 1 implies that a wild-type cell continuously compares the stimulus experienced during the past second with that experienced during the previous 3 sec and responds to the difference (14). This allows the cell to recover from a small step stimulus within 4 sec (Fig. 2). Strains lacking the methylation and demethylation enzymes respond just as rapidly, but they recover much more slowly (Figs. 4 and 5); the kinetics of the events that link the receptors to the flagella appear to be normal, but adaptation is defective (cf. ref. 22).

Stock *et al.* (23), on the basis of studies of migration of methylation-defective cells on swarm plates or in capillary assays, concluded that rapid (second-to-second) adjustments to small changes in concentration occur in the absence of methylation and demethylation. No such adjustments were evident in our data for strains deleted for *cheRcheB* (Figs. 4 and 5). Gradual (minute-to-minute) adjustments still occur, at least for some cells, but they are not complete (Fig. 5). Partial adaptation on the latter time scale also was reported by Stock *et al.* (24) and by Weis and Koshland (25).

The iontophoretic step stimuli used in the experiments of Fig. 4*B* lasted at most 12 sec, about the time required to exchange the medium in the flow cell (Fig. 5). However, iontophoretic step stimuli of 60 sec duration were used in studies of the responses of markers on filamentous *cheRcheB* cells (26), with no sign of adaptation. But it might be that filamentous cells are different, because they have a much larger cytoplasmic space. The matter deserves further study. In any case, it would be of interest to know the rate of migration expected for cells that adapt in the manner shown in Fig. 5. Could it be that this adaptation can account for the small chemotactic rings observed for cells deleted for *cheRcheB* (14, 23)?

We envisage that the following biochemical events occur during the wild-type impulse response (Fig. 1). The concentration of attractant at the cell surface increases a few milliseconds after the pipette is turned on. The attractant binds to the receptors, triggering a signal that raises the flagellar bias and stimulates receptor methylation. When the pipette is turned off, the concentration of attractant rapidly decreases; the attractant leaves the receptors and diffuses away, but the signal persists. The imbalance between receptor occupancy and methylation eventually causes the signal to fall below its prestimulus value. This lowers the bias below its prestimulus level and stimulates demethylation. Finally, as methylation returns to its original level, the signal follows suit, and the bias returns to its prestimulus level. In cheRcheB mutants (Fig. 4), the signal is generated as before, but methylation does not occur. Thus, once the signal passes its peak value, both the signal and the bias drop monotonically to their prestimulus levels. A small but long-lived undershoot would be sufficient to accommodate the data of Fig. 5, which shows partial recovery in bias over a period of 2 min.

From studies of signal propagation in filamentous cells (some containing *cheZ* mutations; ref. 26), we argued that the

Table 1. Transition rates between CW and CCW states for the impulse and step responses shown in the figures

Strain	Fig.	Rate CW → CCW (k_t, sec^{-1}) Initial	Rate CW → CCW (k_t, sec^{-1}) Extreme*	Rate CCW → CW (k_r, sec^{-1}) Initial	Rate CCW → CW (k_r, sec^{-1}) Extreme*
Wild type	1	1.4	≈9	0.8	0.1
	2	1.7	2.6	0.9	0.3
cheRcheB	4*A*	0.8	≈5	1.7	0.1
	4*B*	0.9	2.6	4.1	1.6
	5	0.3	0.7	2.2	0.2
cheZ	6*A*	1.6	2.7	2.8	1.6
	6*B*, up	1.5	3.4	2.2	1.3
	6*B*, down	2.4	1.1	1.5	2.4

Data were computed and plotted as for figure 9 of ref. 14; approximate values were read from the plots by eye. Recall that at equilibrium the mean CW interval is $1/k_t$, the mean CCW interval is $1/k_r$, and the mean bias is $k_t/(k_t + k_r)$.

*For impulse responses (Figs. 1, 4*A*, and 6*A*), the extreme values are for the peak of the first lobe. For the flow-cell experiment (Fig. 5), the extreme values are for the first 20 sec after the flow.

signal that couples the receptors to the flagella could be a protein that is reversibly modified, possibly cheY (see also refs. 27 and 28), and that the *cheZ* gene product is involved in the modification process. When *cheZ* is defective, the rate of decay of the signal appears to be substantially reduced (as in Fig. 6). Normally, both the production and inactivation of the signal must occur on the time scale of roughly 1 sec, since both wild-type and *cheRcheB* cells respond to increases or decreases in attractant concentration within this time span (Figs. 1, 2, and 4). Stock *et al.* (24) have suggested that the slow partial adaptation that they observed in *cheRcheB* pseudorevertants might be due to the kinetics of turnover of the signal. Clear evidence against this possibility is the rapid return of the bias to baseline in cheRcheB mutants following removal of attractant (Fig. 4*B*).

The gain of the system is prodigious: a step change in concentration of L-aspartate (or α-methyl-DL-aspartate) that increases the occupancy of the receptors by 1 molecule (1 part in 600, assuming 600 copies of the receptor protein Tar per cell; cf. ref. 29) transiently increases the rotational bias by ≈0.1. A ramp that increases the receptor occupancy by as little as 1 molecule per sec leads to a steady-state increase in bias of a similar magnitude. A comparison of these data with those of Brown and Berg (13) shows that this increase corresponds to a change in run length by a factor of ≈3.

We thank M. Patricia Conley for carrying out the flow-cell experiments. This work was supported by National Institutes of Health Grant AI16478. Figs. 1, 2, and 4*A* were constructed from a large set of stimulus–response records, subsets of which were described earlier (figures 3*A*, 4, and 7*A*, respectively, of ref. 14). Figs. 1 and 3*B* were included in a lecture given at a NATO Advanced Study Institute (30).

1. Adler, J. (1969) *Science* **166,** 1588–1597.
2. Larsen, S. H., Reader, R. W., Kort, E. N., Tso, W.-W. & Adler, J. (1974) *Nature (London)* **249,** 74–77.
3. Macnab, R. M. & Ornston, M. K. (1977) *J. Mol. Biol.* **112,** 1–30.
4. Berg, H. C. & Brown, D. A. (1972) *Nature (London)* **239,** 500–504.
5. Hazelbauer, G. L. & Harayama, S. (1983) *Int. Rev. Cytol.* **81,** 33–70.
6. Adler, J. (1966) *Science* **153,** 708–716.
7. Macnab, R. & Koshland, D. E., Jr. (1972) *Proc. Natl. Acad. Sci. USA* **69,** 2509–2512.
8. Spudich, J. L. & Koshland, D. E., Jr. (1975) *Proc. Natl. Acad. Sci. USA* **72,** 710–713.
9. Berg, H. C. & Tedesco, P. M. (1975) *Proc. Natl. Acad. Sci. USA* **72,** 3235–3239.
10. Adler, J. (1973) *J. Gen. Microbiol.* **74,** 77–91.
11. Dahlquist, F. W., Lovely, P. & Koshland, D. E., Jr. (1972) *Nature (London) New Biol.* **236,** 120–123.
12. Dahlquist, F. W., Elwell, R. A. & Lovely, P. S. (1976) *J. Supramol. Struct.* **4,** 329–342.
13. Brown, D. A. & Berg, H. C. (1974) *Proc. Natl. Acad. Sci. USA* **71,** 1388–1392.
14. Block, S. M., Segall, J. E. & Berg, H. C. (1982) *Cell* **31,** 215–226.
15. Block, S. M., Segall, J. E. & Berg, H. C. (1983) *J. Bacteriol.* **154,** 312–323.
16. Segall, J. E., Manson, M. D. & Berg, H. C. (1982) *Nature (London)* **296,** 855–857.
17. Berg, H. C. (1983) *Random Walks in Biology* (Princeton Univ. Press, Princeton, NJ).
18. Parkinson, J. S. & Houts, S. E. (1982) *J. Bacteriol.* **151,** 106–113.
19. Berg, H. C. & Block, S. M. (1984) *J. Gen. Microbiol.* **130,** 2915–2920.
20. Parkinson, J. S. (1978) *J. Bacteriol.* **135,** 45–53.
21. Parkinson, J. S. & Parker, S. R. (1979) *Proc. Natl. Acad. Sci. USA* **76,** 2390–2394.
22. Springer, M. S., Goy, M. F. & Adler, J. (1979) *Nature (London)* **280,** 279–284.
23. Stock, J., Borczuk, A., Chiou, F. & Burchenal, J. E. B. (1985) *Proc. Natl. Acad. Sci. USA* **82,** 8364–8368.
24. Stock, J., Kersulis, G. & Koshland, D. E., Jr. (1985) *Cell* **42,** 683–690.
25. Weis, R. M. & Koshland, D. E., Jr. (1986) *Biophys. J.* **49,** 20a (abstr.).
26. Segall, J. E., Ishihara, A. & Berg, H. C. (1985) *J. Bacteriol.* **161,** 51–59.
27. Ravid, S. & Eisenbach, M. (1984) *J. Bacteriol.* **158,** 222–230.
28. Clegg, D. O. & Koshland, D. E., Jr. (1984) *Proc. Natl. Acad. Sci. USA* **81,** 5056–5060.
29. Clarke, S. & Koshland, D. E., Jr. (1979) *J. Biol. Chem.* **254,** 9695–9702.
30. Berg, H. C. (1985) in *Sensory Perception and Transduction in Aneural Organisms*, eds. Colombetti, G., Lenci, F. & Song, P.-S. (Plenum, New York), pp. 19–30.